http://dx.doi.org/10.5012/bkcs.2013.34.12.3641

Collision-induced Energy Transfer and Bond Dissociation in Toluene by H_2/D_2

Jongbaik Ree,[*] Yoo Hang Kim,[†] and Hyung Kyu Shin[‡]

Department of Chemistry Education, Chonnam National University, Gwangju 500-757, Korea. [*]E-mail: jbree@jnu.ac.kr
[†]Department of Chemistry, Inha University, Incheon 402-751, Korea
[‡]Department of Chemistry, University of Nevada, Reno, Nevada 89557, USA
Received August 15, 2013, Accepted September 12, 2013

Energy transfer and bond dissociation of C-H_{methyl} and C-H_{ring} in excited toluene in the collision with H_2 and D_2 have been studied by use of classical trajectory procedures at 300 K. Energy lost by the vibrationally excited toluene to the ground-state H_2/D_2 is not large, but the amount increases with increasing vibrational excitation from 5000 and 40,000 cm^{-1}. The principal energy transfer pathway is vibration to translation (*V-T*) in both systems. The vibration to vibration (*V-V*) step is important in toluene + D_2, but plays a minor role in toluene + H_2. When the incident molecule is also vibrationally excited, toluene loses energy to D_2, whereas it gains energy from H_2 instead. The overall extent of energy loss is greater in toluene + D_2 than that in toluene + H_2. The different efficiency of the energy transfer pathways in two collisions is mainly due to the near-resonant condition between D_2 and C-H vibrations. Collision-induced dissociation of C-H_{methyl} and C-H_{ring} bonds occurs when highly excited toluene (55,000-70,400 cm^{-1}) interacts with the ground-state H_2/D_2. Dissociation probabilities are low (10^{-5}~10^{-2}) but increase exponentially with rising vibrational excitation. Intramolecular energy flow between the excited C-H bonds occurring on a subpicosecond timescale is responsible for the bond dissociation.

Key Words : Collision-induced, Dissociation, Intramolecular energy flow

Introduction

Studies on the rates and mechanisms of energy transfer in molecular collisions are critical to understanding elementary processes which play a vital role in chemical reactions.[1-13] The collision-induced relaxation of vibrationally excited polyatomic molecules is of particular interest as it directly affects the fate of bond dissociation and subsequent reaction dynamics. Energy transfer involving polyatomics has been studied experimentally by a variety of techniques. Experimental studies have been commonly carried out using time-resolved infrared flourescence (TR-IRF)[4-6] or ultraviolet absorption (UVA) techniques.[7-9] Several studies have used techniques based on photothermal processes.[10-12] Through these studies the researchers have provided insight into relative collision efficiencies and their dependence on the energy of excited molecules. Recently, Hsu *et al.* have studied the energy transfer of highly vibrationally excited molecules using crossed-beam techniques.[13] However, theoretical studies of energy transfer processes in polyatomic molecules have lagged behind the experimental studies as models and collision dynamics of many-body interactions are difficult to develop.[14-22] When such studies are developed using physically realistic interaction models, the results can complement experimental studies and guide future studies.

In collisions involving a large organic molecule, the average amount of energy transfer per collision is not very large.[23-31] One such molecule is toluene, which contains two distinctly different C-H bonds, namely the methyl C-H and ring C-H bonds, along with many C-C bonds. When toluene undergoes a collision with other molecules, both intermolecular energy transfer and intramolecular energy flow from one CH bond to others *via* C-C bonds can occur.[22,31] Hippler and co-workers studied the deactivation of the excited toluene by about 60 different collider gases using the UVA techniques to follow the collisional relaxation of cycloheptatriene.[32] They prepared highly vibrationally excited toluene (52,000 cm^{-1} = 150 kcal/mol) after irradiating cycloheptatriene and showed the excited molecule dissociates into benzyl radical and H atom, which indicate that the extent of energy transfer can be significant. Toselli and co-workers investigated the collisional loss of vibrational energy from gas-phase toluene by 20 collider gases by monitoring the TR-IRF from the C-H stretch modes near 3.3 mm.[23] Computational studies of collision-induced energy transfer between aromatic polyatomic molecules including toluene have been reported by Bernshtein and Oref.[33]

The purpose of this paper is to study energy transfer and bond dissociation in the collision of highly vibrationally excited toluene with H_2 and D_2 using quasiclassical trajectory procedures. We use the model presented in Ref. 22, where the toluene + N_2/O_2 collision was considered. In the present systems, toluene is in interaction with the light molecules, which create a collision environment greatly different from that of N_2 or O_2. The vibrational frequencies are now more than twice those of the latter molecules, thus making the contribution of intermolecular vibrational energy transfer more significant. In particular, the vibrational frequency of D_2 is very close to C-H frequency in toluene, creating the near-resonant condition which can lead to increased vibra-

tional energy transfer. The low moments of inertia of H_2/D_2 lead larger rotational spacings, which in turn lead to a significant contribution of rotational energy transfer. The masses of these molecules are low, so the collision dynamics can be significantly different from that involving heavier masses such as N_2/O_2. Further, a comparative study of toluene + H_2 and toluene + D_2 is important as it can reveal the effects of isotopic substitutions on the transfer of energy and bond dissociation in large molecules. To study these aspects, we start with a vibrationally excited toluene (5000-40,000 cm^{-1}) and determine energy transfer between toluene and H_2/D_2 as a function of the toluene vibrational energy content and compare the results with experimental data. Energy transfer processes occurring in the collision are vibration-to-translation (*V-T*), vibration-to-rotation (*V-R*) and vibration-to-vibration (*V-V*) pathways. We then take highly excited toluene (55,000-70,400 cm^{-1}) to study its collision dynamics with H_2/D_2 leading to bond dissociation with particular emphases on the importance of intramolecular energy flow between the excited methyl and ring C-H bonds. Dissociation of ring C-H or methyl C-H can occur when the initial energy stored in the molecule redistribute intramolecularly on collision, the process which will be discussed in detail.

Interaction Model and Energies

The model and internal coordinates of toluene have been reported in Ref. 22 for the collision of toluene with N_2/O_2 and the same interaction model will be adopted here whenever applicable. We briefly recapitulate the essential aspects of the model for clarity using the same notations and conventions used in Ref. 22. We describe the collision of toluene with hydrogen molecule in terms of 39 intramolecular coordinates of the planar ring and the rotational and vibrational modes of the incoming molecule. Toluene is considered to be non-rotating during the collision.

The C-H_{ring} bond is in the clockwise side from C-H_{methyl}. The internal modes of toluene are 6 stretches (x_1, x_2, x_3, x_4, x_{14}, x_{15}) and 12 bends (ϕ_1, ϕ_2, ϕ_3, ϕ_4, ϕ_5, ϕ_6, ϕ_7, ϕ_1', ϕ_1'', ϕ_b, ϕ_b', ϕ_b'') between C-H_{ring} and C-H_{methyl}, the region we consider to be the interaction (or primary) zone, where the C-H_{methyl} and C-H_{ring} bonds are in the direct interaction with H_2; see Figure 1. Other coordinates included are the x_5-x_9 $(C\text{-}C)_{ring}$ stretches, x_{10}-x_{13} $(C\text{-}H)_{ring}$ stretches and ϕ_8-ϕ_{19} bends around the carbon atoms C_3, C_4, C_5 and C_6, a total of 9 stretches and 12 bends, in the region remote from the primary zone. We refer this region as the secondary zone.

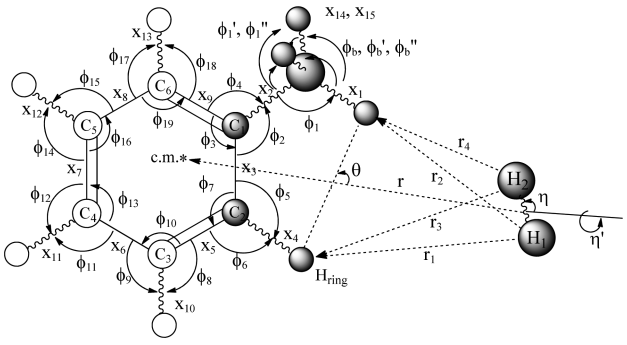

Figure 1. Collision model. The stretching and bending coordinates of vibrations are defined. All carbon atoms and ring H atoms are coplanar and modes are numbered clockwise. The star denotes the center-of-mass (c.m.) of toluene. The displacement of each vibrational coordinate is identified by $x_{e1} + x_1$, *etc.* (see the text).

The interaction energies needed to describe the collision of H_2 with toluene must contain terms responsible for the coupling of the relative motion with the ring C-H stretch and methyl group C-H stretch as well as the coupling between the stretches and bends. We first identify the two atoms of H_2 as $H_{(1)}$ and $H_{(2)}$ and denote the interatomic distances r_1-r_4 as shown in Figure 1, where r represents the distance between the center-of-mass (c.m.) of H_2 and the c.m. of toluene describing the relative motion of the collision system. The interatomic distances can be expressed in terms of the instantaneous coordinates of the C-H_{methyl} bond, C-CH_{methyl} bond, $(C\text{-}C)_{ring}$ bond, C-H_{ring} bond, C-C-H_{methyl} bend, C-C-C_{methyl} bend, C-C-H_{ring} bend and H-H bond. That is, $r_i = r_i(r, x_1, x_2, x_3, x_4, \phi_1, \phi_2, \phi_5, x, \theta, \eta, \eta')$ for i = 1-4, where x is the displacement of the H_2 bond from its equilibrium distance d, and θ is the angle of incidence defined in Figure 1, η and η' are the rotational angles of H_2. These atom-atom distances are given in Ref. 22. The coupling of these modes with others including those of the inner zone will have to be considered in formulating the overall interaction energy.

The overall interaction energy is the sum of the Morse-type intermolecular terms, Morse-type stretching terms and the harmonic bending terms of toluene, intramolecular coupling terms, the incident molecule's term and London interaction,

$$V = \Sigma U(r_\beta) + U_s(x_i) + U_b(\phi_j) + U_{\text{int}}(Y_i Y_j) + U_{inc}(x, \eta, \eta') + \frac{-3I_1I_2}{2(I_1+I_2)}\frac{\alpha_1\alpha_2}{r^6} \quad (1)$$

where,

$$U(r_\beta) = D[e^{-(r_{e\beta}-r_\beta)/a} - 2e^{(r_{e\beta}-r_\beta)/2a}],\ \beta = 1\text{-}4$$

$$U_s(x_i) = \Sigma D_i[1-e^{-x_i/b_i}]^2,\ i = 1\text{-}15$$

$$U_b(\phi_j) = \frac{1}{2}\Sigma k_j\phi_j^2,\ j = 1\text{-}24$$

$$U_{\text{int}}(Y_iY_j) = \Sigma K_{ij}(Y_i - Y_{ei})(Y_j - Y_{ej}),\ i \neq j$$

$$U_{inc}(x, \eta, \eta') = D_{inc}[1-e^{-x/b_{inc}}]^2 + \frac{1}{2}I_{inc}\dot{\eta} + \frac{1}{2}I_{inc}\dot{\eta}'.$$

The values of potential and spectroscopic constants for toluene are listed in Table 1.[34-41] Each bond length will be denoted by $(x_{ei} + x_i)$, where x_i is the displacement of the bond length from its equilibrium value x_{ei}. Similarly, we express each bending coordinate as $(\phi_{ej} + \phi_j)$, where ϕ_j is the displacement of the jth bending vibration from the equilibrium angle ϕ_{ej}. In the London term, I_i is the ionization potential and α_i is the polarizability of toluene and H_2/D_2. The "inc" in

Table 1. Potential and spectroscopic constants for toluene

Stretches[#]	CH, i = 4, 13	CH, i = 10, 11, 12	CC, i = 3, 9	CC, i = 5, 6, 7, 8	C-CH_3, i = 2	CH_{methyl}, i = 1, 14, 15
Dissociation energy, D_{oi} (eV)	4.762[a]	4.554[b]	5.308[a]	5.638[b]	4.337[a]	3.782[a]
Bond distance, d_i (Å)	1.098[c]	1.077[b]	1.398[c]	1.394[b]	1.509[c]	1.145[c]
Frequency (cm^{-1})	3144[d]	3170[f]	1494[d]	1605[e]	1208[d]	3060[d]
Range parameter (Å)	0.541	0.526	0.468	0.449	0.523	0.498
Bends	ϕ_1, ϕ_1', ϕ_1''	ϕ_2, ϕ_4	ϕ_3	ϕ_i = 5,6,8,9,11, 12,14,15,17,18	ϕ_i = 7,10,13,16,19	ϕ_b, ϕ_b', ϕ_b''
Frequency (cm^{-1})	1460[e]	344[e]	521[e]	1312[e]	623[e]	1384[b]
Bond angle (Å)[e]	107.6	120	120	120	120	109.5
Force constant (J $rad^{-2} \times 10^{-18}$)[e]	0.667	0.732	1.043	0.521	1.065	0.561

[#]Number i represents the subscript of the vibrational cooridinate x shown in Figure 1. [a]Reference 34-36. [b]reference 37. [c]reference 38; the dissociation energy D_i used throughout the paper including Eq. (1) is $D_i = D_{oi} + \frac{1}{2}\hbar\omega_{ei}$. [d]reference 39, 40. [e]reference 41. [f]reference 40

Eq. (1) means the incident molecule, H_2 or D_2. For the intermolecular interaction, we take $D = 116.85k_B$ and $126.94k_B$ for toluene + H_2 and toluene + D_2, respectively, the Lennard-Jones (LJ) parameter for the well depth for the collision pairs calculated by the usual combining rule,[42] where k_B is the Boltzmann constant, and a = 0.238 and 0.235 Å for toluene + H_2 and toluene + D_2, respectively.[41,42] For the ith stretch, we use $b_i = (2D_i/\mu_i\omega_i^2)^{1/2}$, where $D_i = D_{o,i} + \frac{1}{2}\hbar\omega_{ei}$, to determine the exponential range parameters listed in Table 1. In the coupling terms, $Y_i = x_i$ or ϕ_i and the coupling constant K_{ij} are taken from Xie and Boggs' *ab initio* calculations.[43] Table 2 lists the potential and spectroscopic constants for H_2 and D_2.[44-46]

The equations of motion which determine the time evolution of the relative motion, 15 stretches, 24 bends and three motions of the incident molecule for the given incident angle can be expressed in the general forms as

$$M_k d^2q_k(t)/dt^2 = -\partial/\partial q_k V(r, x_1\text{-}x_{15}, \phi_1\text{-}\phi_{24}, x, \eta, \eta', \theta); \quad k = A, B, C, x, \eta, \eta', \tag{2}$$

where $k = A$ for the relative motion with the reduced mass $M_A = \mu$, $k = B$ for the vibrations x_1-x_{15} with the corresponding reduced mass $M_B = \mu_i$, $k = C$ for the bending modes ϕ_1-ϕ_{24} and the moment of inertia $M_C = I_j$. For the incident molecule, $k = x$, η and η' are associated with the reduced mass μ_{inc} and the moment of inertia I_{inc}. We use the standard numerical routines[47,48] to integrate these equations for the initial conditions at $t = t_o$ and their conjugate quantities $dr(t_o)/dt$, $dx_i(t_o)/dt$, $d\phi_j(t_o)/dt$, $dx(t_o)/dt$, $d\eta(t_o)/dt$, and $d\eta'(t_o)/dt$, where the derivatives are evaluated at $t = t_o$. The initial conditions for the relative and vibrational motions in the interaction zone are given in Ref. 29. We sample 40,000 trajectories for each run at 300 K, where the sampling includes determining collision energies (E) sampled from the Maxwell distribution and weighting the initial vibrational and rotational energies by the Boltzmann distribution at 300 K.

Table 2. Potential and spectroscopic constants for toluene, H_2 and D_2

Molecule	toluene	H_2	D_2
Ionization energy, I (eV)[a]	8.828	15.4259	15.4666
Polarizability, (Å^3)	9.906[a]	0.787[b]	0.782[b]
Dissociation energy, D_{oi} (eV)[c]		4.478	4.556
Bond distance, d_i (Å)[c]		0.741	0.742
Vibrational frequency (cm^{-1})[c]		4401.21	3115.50
Range parameter, b (Å)[d]		0.257	0.257

[a]Reference 44; the ionization energy and polarizability of toluene are shown here for easy comparison with the corresponding values of H_2 and D_2. [b]reference 45. [c]reference 46. [d]range parameter is determined from the relation $b_i = (2D_i/\mu_i)^{1/2}/\omega_i$.

The principal quantity we determine in non-dissociative cases is the difference between the initial and final energies of translation, rotation and vibration of H_2 (or D_2). We denote the ensemble-averaged energy transfer by $\langle\Delta E\rangle = \langle E_{final} - E_{initial}\rangle$ such that a positive value represents an energy loss by toluene *via* the *V-T*, *V-V* and *V-R* pathways. In studying dissociative cases, we determine the time evolution of methyl and ring C-H bonds, and sum all trajectories, which lead to the methyl or ring C-H energy reaching its dissociation threshold. We discuss the latter process in terms of collision-induced intramolecualr energy flow.

Results and Discussion

Energy Loss by Toluene. In Figure 2(a), we show the dependence of energy loss by toluene on the total vibrational energy of toluene E_T in the toluene + H_2 collision at 300 K. Plotted is the E_T dependence of the amount of energy transfer from toluene to H_2 *via V-T*, *V-V*, *V-R* pathways, as well as their sum. The lowest value of E_T considered in this figure is 6204 cm^{-1} or 0.769 eV, which is equivalent to the sum of one-quantum vibrational energies of C-H_{methyl} and C-H_{ring} 3060 cm^{-1} (0.379 eV) and 3144 cm^{-1} (0.390 eV), respectively. We treat the incident molecules to be in the ground state, so the initial energies are ½(4401) and ½(3115) cm^{-1} for H_2 and D_2, respectively. (We give energies in both cm^{-1} and eV for convenience.) At the lowest value of E_T, the energy loss is −6 cm^{-1} [see "sum" in Figure 2(a)], which is obtained by adding 13, −26 and 7 cm^{-1} for *V-T*, *V-V* and *V-R*, respectively. When E_T is raised from 6204 cm^{-1} to 37,221 cm^{-1}, the range considered in experimental studies,[23] the

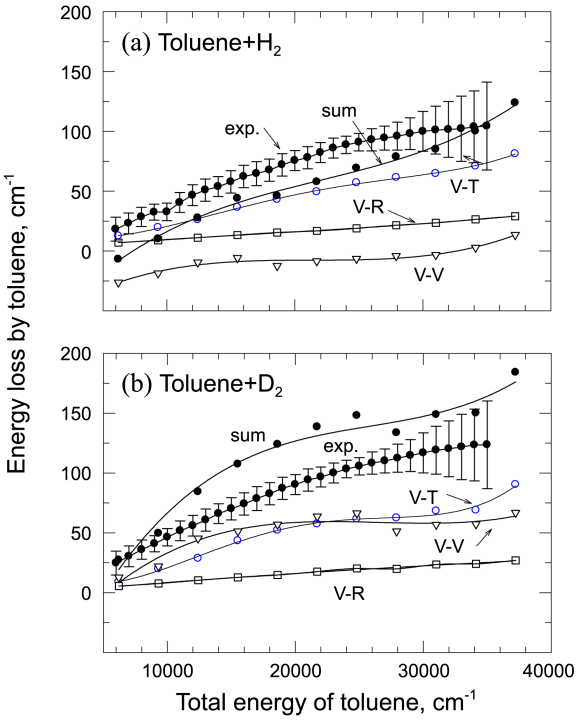

Figure 2. Plots of energy loss by toluene *vs*. total energy of toluene: (a) Toluene + H_2 and (b) toluene + D_2. In each frame, the transfer of vibrational energy from toluene to various motions of H_2/D_2 (*i.e*, *V-T*, *V-R* and *V-V*) is indicated. The sum of all three contributions indicated by "sum" is compared with the experiment data.[23]

amount of energy transfer varies from −6 cm^{-1} to 123 cm^{-1}, which is less than 1% of E_T. At the risk of repetition: positive energy, such as 123 cm^{-1}, represents the energy loss by toluene. The maximum energy content 37,221 cm^{-1} considered in Figure 2(a) is the sum of C-H_{methyl} and C-H_{ring} energies, which are taken to be 18,359 cm^{-1} (2.276 eV) and 18,862 cm^{-1} (2.339 eV) respectively. The experimental data plotted in Figure 2(a) are the work of Toselli *et al*. obtained from the measurements of collisional loss of vibrational energy by use of the time-resolved infrared fluorescence from the C-H stretch modes near 3.3 μm.[23] The energy loss gradually increases with increasing E_T as found in the computed sum. The latter variation is known to be a general behavior for the relaxation of toluene by rare gases and diatomic molecules in both experimental and theoretical studies.[16,17]

A particularly important aspect of the present result is that we can identify the contributions of individual energy transfer pathways to the vibrational relaxation of toluene. As shown in Figure 2(a), the *V-V* values are negative except near the upper end of E_T. The *V-V* curve rises from −26 cm^{-1} at E_T = 6204 cm^{-1} to −3 cm^{-1} at the toluene energy content as high as E_T = 31,018 cm^{-1}. As the negative values indicate toluene gains energy, the *V-V* pathway does not contribute to the relaxation of excited toluene. On the other hand, the amount of *V-T* energy transfer is positive and significant over the entire E_T range. In fact, H_2 removes energy from toluene by 13 cm^{-1} at E_T = 6204 cm^{-1} to 81 cm^{-1} at E_T = 37,221 cm^{-1}, the *V-T* process being the leading pathway for the relaxation process. We note that the *V-R* value shown in Figure 2(a) is always positive, but its contribution to the sum is minor.

The plots similar to Figure 2(a) are presented in Figure 2(b) for toluene + D_2. The collision system now involves a heavier incident molecule with a lower force constant. The reduced mass affecting the relative motion of the collision system is now $\mu \approx \mu_{D2}$ which is twice the reduced mass $\mu \approx \mu_{H2}$ of the toluene + H_2 system. The vibrational frequency of D_2 is 3115 cm^{-1}, which is very close to the C-H frequencies (C-H_{methyl} = 3144 cm^{-1} and C-H_{ring} = 3060 cm^{-1}). Such near resonant condition enhances *V-V* energy flow. Thus we find the *V-V* pathway is more efficient than in toluene + H_2. Unlike the toluene + H_2 case, the amount of *V-V* energy transfer is now always positive; see Figure 2(b). It increases from 13 cm^{-1} at E_T = 6204 cm^{-1} to 67 cm^{-1} at E_T = 37,221 cm^{-1}, which are comparable to the *V-T* values. The contribution of *V-R* pathway is insignificant as in the toluene + H_2 system. As shown in Figure 2(b), the magnitude of energy loss indicated by "sum" is larger than the observed values[23] but the E_T dependence is in fair agreement. The comparison of Figures 2(a) and 2(b) indicates that the heavier D_2 with a frequency in near resonance with the C-H bonds is more efficient in relaxing the highly vibrationally excited toluene. Thus increased efficiency of *V-T* and *V-V* energy transfer in toluene + D_2 is the manifestation of the effects of mass and frequency.

Figure 3 shows the effects of vibrational excitation of H_2/D_2 on the energy loss of toluene by assigning the energies

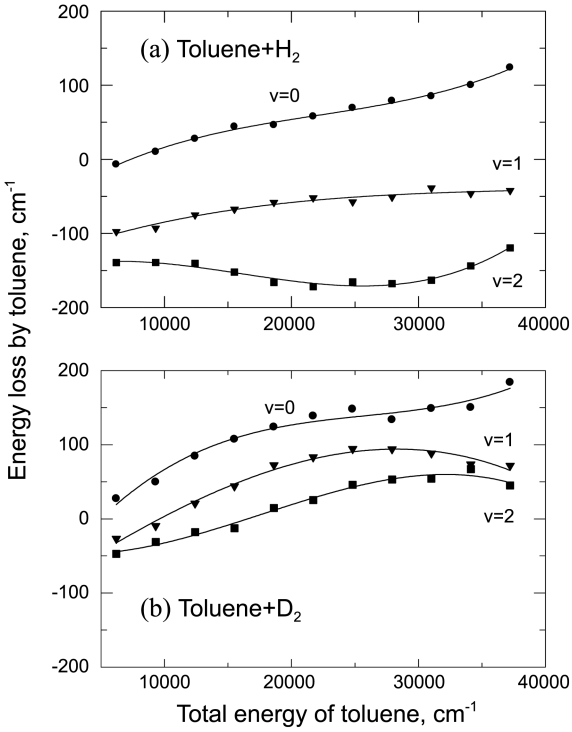

Figure 3. Dependence of "sum" on the vibrational excitation (v = 0 – 2) of the incident molecules: (a) toluene + H_2 and (b) toluene + D_2.

equivalent to one and two quanta to H_2/D_2; see $v = 1$ and 2 curves in Figures 3(a) and 3(b). The $v = 0$ results are the "sum" curves reproduced from Figures 2(a) and 2(b). The $v = 1$ and 2 curves of H_2 clearly represent the incident molecule losing its energy to the target. The extent of H_2 to toluene energy transfer increases with increasing the vibrational excitation of H_2, which is mainly due to the contribution of the *V-V* energy pathway working in the direction of H_2 to toluene. A similar trend of energy transfer decreasing with increasing vibrational excitation is seen in Figure 3(b) for toluene + D_2 but the process now transfers energy from toluene to D_2 except at the lower end of E_T.

Dynamics of Bond Dissociation. When the internal state of a highly vibrationally excited toluene is perturbed by H_2/D_2, either C-H_{methyl} or C-H_{ring} bond can dissociate. We discuss important characteristics of the dissociation dynamics in this section. The results presented in Figure 2 suggest collision-induced bond dissociation is not likely to occur for toluene

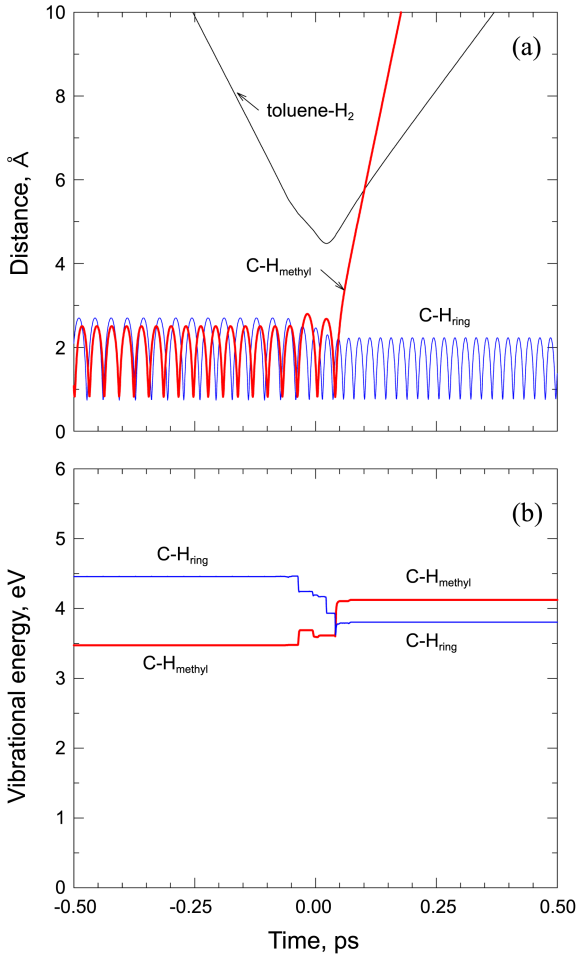

Figure 4. The dynamics of a representative trajectory of the C-H_{methyl} bond dissociation in toluene + H_2 collision: (a) Time development of toluene-H_2, C-H_{methyl} and C-H_{ring} distances, (b) Time development of C-H_{methyl} and C-H_{ring} vibrational energies. The total energy of toluene above the ground state E_T is 63,944 cm^{-1} (7.928 eV), which is distributed between C-H_{methyl} and C-H_{ring} such that the energy of each bond is 0.50 eV below the dissociation threshold. The collision energy E taken from the Maxwell sampling is 0.070 eV.

with low to medium extent of vibrational excitation. Thus we take a sufficiently high vibrational energy state of toluene. For the representative trajectory shown in Figure 4, the C-H_{methyl} and C-H_{ring} bonds start out with energies 3.472 eV and 4.457 eV, respectively, 0.50 eV below the dissociation threshold, while other bonds and bends are initially in the ground state. In Figure 4(a), we show the time evolution of the toluene-H_2 distance, which is the collision trajectory, the C-H_{methyl} and C-H_{ring} distances.

The incident H_2 molecule is in the ground state, so it acts primarily as a perturber inducing energy flow from one C-H bond to another. The collision time is scaled such that the instant of the initial impact is zero. For the representative trajectory chosen, H_2 approaches toluene to the closest separation 4.30 Å with the collision energy $E = 0.070$ eV. The C-H_{methyl} bond begins to be perturbed at $t \approx -0.1$ ps, when energy starts to flow from the C-H_{ring} bond; see Figure 4(b). During this subpicosecond time period, main part of the energy lost by the C-H_{ring} bond passes through the x_3 and x_2 C-C bonds and eventually localizes in the C-H_{methyl} bond for its dissociation. As shown in Figure 4(b), the amount of energy lost by the C-H_{ring} bond is 0.654 eV, whereas the C-H_{methyl} bond gains 0.650 eV, thus exceeding the dissociation threshold. The closeness of the latter two values indicates the energy needed for the dissociation of highly excited C-H_{methyl} comes entirely from C-H_{ring} through intramolecular flow.

Figure 5(a) shows the dynamics of energy flow in toluene + D_2. Intramolecular energy flow and bond dissociation occurs in a time-scale of about 0.6 ps, much longer than 0.1 ps of the toluene + H_2 case. As shown in Figure 5, the excited C-H_{methyl} bond undergoes nearly 20 oscillations before dissociation. It is interesting that such a highly excited C-H_{methyl} bond can remain undissociated so long. The bond waits that long until the last trace of energy needed for dissociation arrives from C-H_{ring}. The detail of energy flow is seen in Figure 5(b). The C-H_{methyl} bond distance begins to be perturbed from its initial vibrational motion as the collision trajectory approaches $t = 0$, when the first impact occurs. The incident molecule remains near toluene for ~0.60 ps, during which the C-H_{methyl} bond first loses a small mount of energy to D_2 and then gains a large amount from C-H_{ring} near the end of collision *via* intramolecular flow. During the period of ~0.6 ps, the C-H_{ring} bond loses energy as high as ~1.5 eV, which flows through C-C bonds. Only about 0.6 eV of the energy reaches the C-H_{methyl} bond, whereas the rest accumulates in C-C stretches and H-C-C, C-C-C bends. Thus the time evolution suggests that it takes about 0.6 ps for the vibrational energy to travel a distance of 2.8 Å for two C-C bonds for bond dissociation in the toluene + D_2 collision. Comparing the curves shown in Figure 4 with those in Figure 5, we can see the dissociation of C-H_{methyl} in toluene + D_2 occurs *via* a long-time, or complex-mode, mechanism. Although it is short, the time scale for bond dissociation in the representative case of toluene + D_2 shows that the dissociation does not occur instantaneously.

As shown in Figures 6 and 7, the collision dynamics

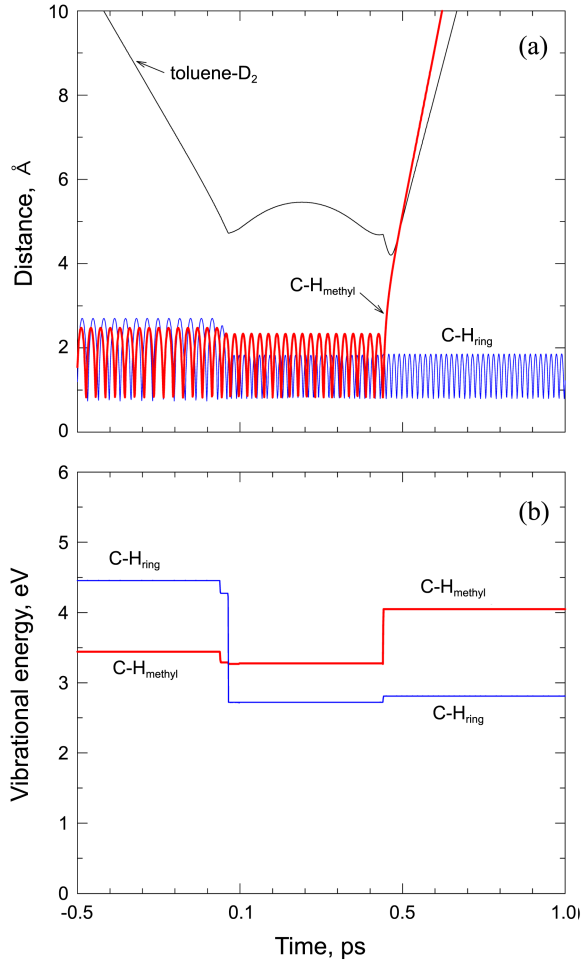

Figure 5. Plots are the same as Figure 4, but they are now for the toluene + D_2 collision. The collision energy E is 0.035 eV.

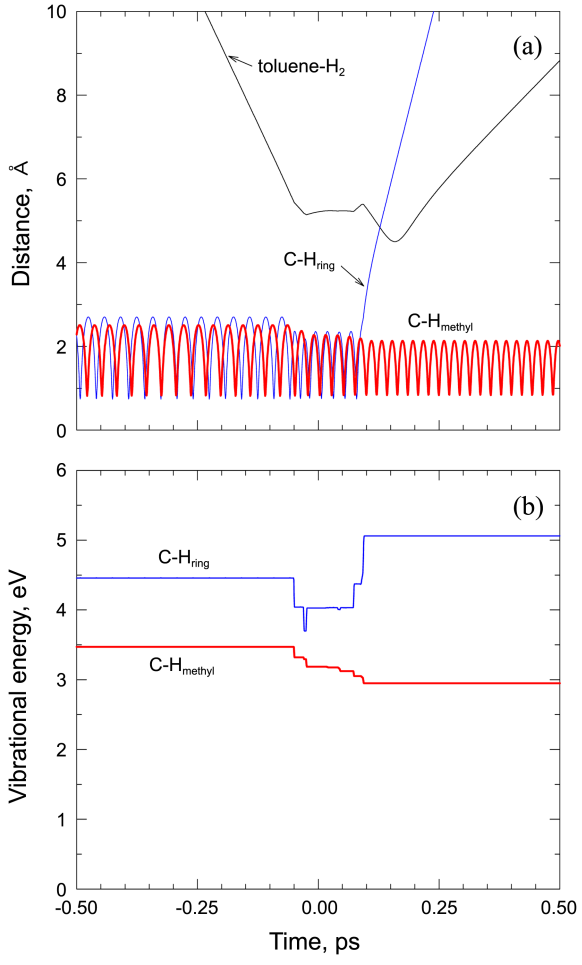

Figure 6. The dynamics of a representative trajectory of the C-H_{ring} bond dissociation in toluene + H_2 collision: (a) Time development of toluene-H_2, C-H_{ring} and C-H_{methyl} distances. (b) Time development of C-H_{ring} and C-H_{methyl} vibrational energies. The total energy of toluene E_T is the same as that given in Figure 4, but the collision energy E is 0.087 eV.

leading to C-H_{ring} dissociation in both toluene + H_2 and toluene + D_2, bond dissociation proceeds through a complex-mode period. In the latter system, the C-H_{ring} bond distance undergoes a large amplitude motion before dissociation; see Figure 7(a). Even in toluene + H_2, the period is nearly 0.3 ps, which is significantly longer than the C-H_{methyl} dissociation case shown in Figure 4(a). As the collision partners interact in the representative trajectory considered in Figure 6(b), both C-H_{methyl} and C-H_{ring} bonds begin to lose energy mainly to C-C bonds and bends intramoleculary, but near the end of complex-mode period, the C-H_{ring} bond gains back most of its energy from C-C bonds and bends, as well as that from C-H_{methyl}. The collision trajectory shown in Figure 6(a) indicates that the benzyl radical and H_2 still undergo another impact as H_{ring} flies away from the primary zone. In the C-H_{ring} dissociation for toluene + D_2 considered in Figure 7(b), the C-H_{methyl} loses its vibrational energy as large as 1.38 eV, part of which flows to C-H_{ring} upon the first impact. The C-H_{ring} bond gains enough energy for dissociation, but the fragmented H_{ring} becomes attracted back to the radical before it has a chance to escape from the primary zone. The large amplitude motion of the C-H_{ring} bond noted above is the manifestation of this recapture period. At the latter period, the rebounding H_{ring} atom gains enough kinetic energy to recede from the reaction zone. We note that in the four representative cases considered in Figures 4-7, the collision energies E are 0.070, 0.035, 0.087 and 0.052 eV, respectively, which lie in the tail of the Maxwell distribution at 300 K.

We find the collisions taking place at or below the most probable velocity (or energy) of the distribution are inefficient in dissociating even for such highly excited C-H bonds. Thus H_2/D_2 approaching toluene with collision energy above the most probable value has a chance to induce intramolecular energy flow to a sufficient extent for bond dissociation.

We plot the dissociation probabilities for toluene + H_2 collision at 300 K in Figure 8(a). The total energy content of highly excited toluene is considered to be localized initially in the C-H bonds as noted above. The initial energy of each bond is maintained below its dissociation threshold value, so that intramolecular energy flow through C-C bonds and bends can lead to dissociation. Dissociation probabilities are found to be low as the light molecules are not efficient in

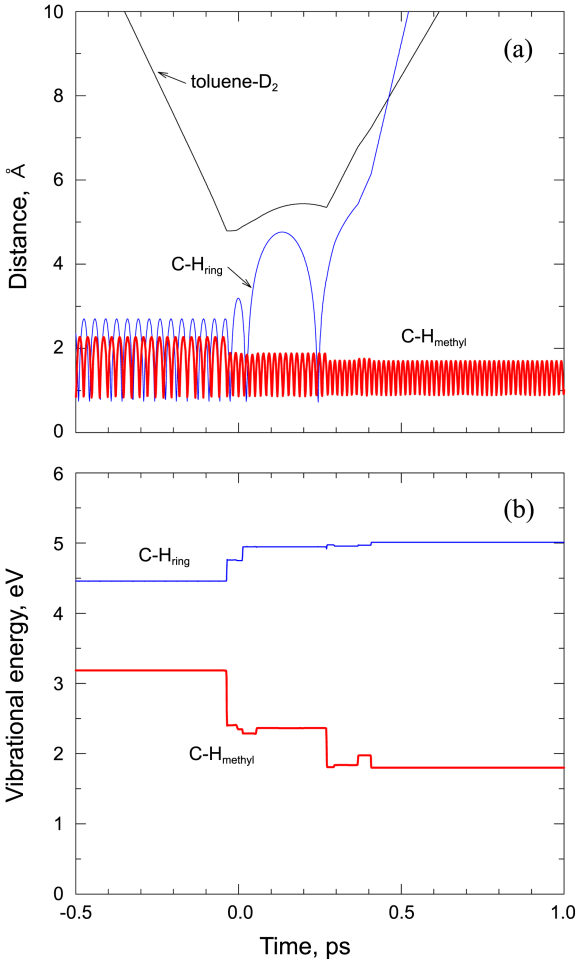

Figure 7. Plots are the same as Figure 6, but they are now for the toluene + D_2 collision. The collision energy E is 0.052 eV.

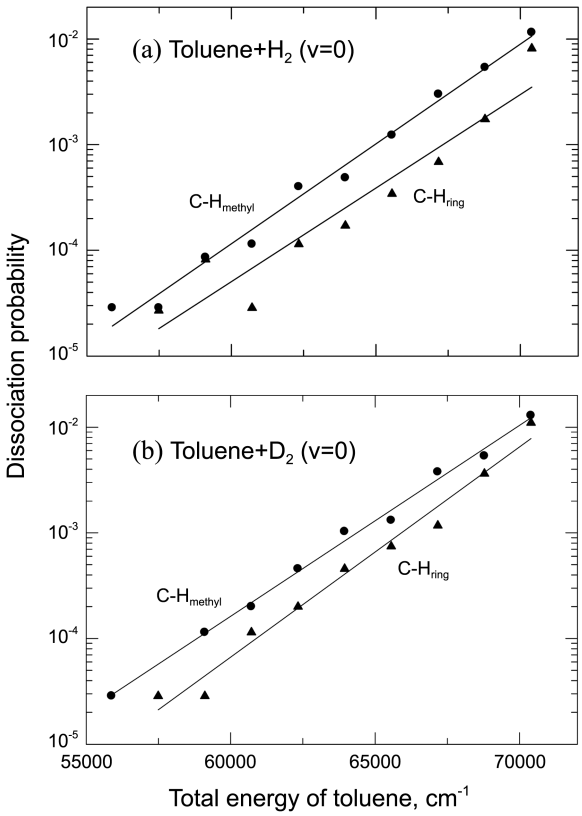

Figure 8. Dissociation probabilities for C-H_{methyl} and C-H_{ring} bonds in (a) toluene + H_2 and (b) toluene + D_2. Both H_2 and D_2 are in the ground state.

inducing intramolecular energy flow from one C-H bond to another. Bond dissociations begin to occur when the total energy content of toluene is gradually raised to 57,492 cm^{-1}, which is partitioned 32,719 cm^{-1} (4.0567 eV) in C-H_{ring} and 24,773 cm^{-1} (3.0715 eV) in C-H_{methyl}. The latter two energies are ~0.9 eV below the dissociation threshold. The semilogarithmic plot shown in Figure 8(a) indicates the dissociation probability is low (~10^{-5}), but rise very rapidly with increasing energy content. At 70,396 cm^{-1}, which is partitioned in the two bonds such that their bond energies are 0.1 eV below the threshold, both probabilities are now ~0.01.

As shown in Figure 8(a), the probability of C-H_{methyl} dissociation is higher than that of C-H_{ring} dissociation over the entire energy range considered. A similar energy dependence of both probabilities is seen for toluene + D_2; see Figure 8(b). The D_2 probabilities are slightly higher than the H_2 case, but the principal qualitative features of the semilogarithmic energy dependence remain unchanged. It is interesting to note that the probabilities of toluene + N_2/O_2 are higher than the present values primarily due to the fact that heavier incident molecules lead to larger extent of intramolecular energy flow.[22]

Concluding Comments

We have studied energy loss by vibrationally excited toluene and dissociation of C-H bonds in the toluene + H_2/D_2 collision systems at 300 K using classical trajectory procedures. The collision system consists of the primary zone of toluene + H_2/D_2 interaction, where the incident molecule interacts with both C-H_{methyl} and C-H_{ring} bonds, and the secondary zone which includes the stretches and bends of toluene beyond the primary zone. Trajectory calculations are carried out for the target molecule with vibrational energy in its two C-H bonds varying from 5000 to 40,000 cm^{-1}, while other stretches and bends are initially in the ground state.

The amount of energy lost by vibrationally excited toluene interacting with the ground-state H_2/D_2 is small, but the energy loss increases when the extent of vibrational excitation increases. The entire energy transfer process taking place on a subpicosecond time scale. The dependence and magnitude of energy loss on the total energy of toluene are in general agreement with experimental data. The amount of energy transfer is significantly larger in toluene + D_2, where C-H and D_2 vibrations are in near resonance. Further, the heavier D_2 imparts stronger perturbation on the C-H bonds, thus enhancing the relaxation process of toluene. The main contribution to the vibrational relaxation of toluene comes from the *V-T* energy transfer pathway in both toluene + H_2 and toluene + D_2 collisions. The *V-V* pathway is inefficient

in toluene + H_2 because of the large disparity in their vibrational frequencies. In general, the *V-R* pathway plays a minor role in the relaxation of toluene. When the incident molecules H_2/D_2 are vibrationally excited (v = 1 and 2), the amount of energy lost by toluene is small compared to the v = 0 case as toluene tends to gain energy from the excited collision partners.

When the total energy content E_T of toluene is sufficiently high, either C-H bond can dissociate in collisions with H_2/D_2 molecule. The time evolution of collision events shows that the dissociation occurs when the internal energy of toluene is initially above 55,000 cm^{-1} (~6.8 eV) and is nearly equally distributed between C-H_{methyl} and C-H_{ring}. Dissociation probabilities are low but rise exponentially with increasing initial energy. Dissociation occurs as a result of the incident molecule (H_2 or D_2) inducing intramolecular energy flow from one C-H bond to another *via* C-C bonds and bends. The dissociation probability of C-H_{methyl} is significantly higher than that of C-H_{ring} as collision-induced energy flow from the high-frequency C-H_{ring} to low-frequency C-H_{methyl} dominates the reverse process. No experimental data are available for C-H bond dissociation of highly excited toluene, but the present values are comparable with those for toluene + N_2 and toluene + O_2 collisions,[22] while they are lower than those of toluene + HF and toluene + Ar.[30,31]

Acknowledgments. This work was financially supported by research fund of Chonnam National University in 2012.

References

1. Cottrell, T. L.; McCoubrey, J. C. *Molecular Energy Transfer in Gases*; Butterworths: London, 1961: experimental data in Ch. 5 and review of theoretical approaches in Ch. 6.
2. Burnett, G. M.; North, A. M., Eds.; *Transfer and Storage of Energy by Molecules*, Vol. 2; Wiley: New York, 1969.
3. Smith, I. W. M. in *Gas Kinetics and Energy Transfer*; Vol. 2, Specialist Periodical Reports; Chemical Society, Burlington House: London, 1977; pp 1-57.
4. Ma, J.; Liu, P.; Zhang, M.; Dai, H.-L. *J. Chem. Phys.* **2005**, *123*, 154306.
5. Poel, K. L.; Alwahabi, Z. T.; King, K. D. *Chem. Phys.* **1995**, *201*, 263.
6. Smith, I. W. M.; Warr, J. F. *J. Chem. Soc. Faraday Trans.* **1991**, *87*, 807.
7. Hippler, H.; Otto, B.; Troe, J. *Ber. Bunsen-Ges. Phys. Chem.* **1989**, *93*, 428.
8. Nakashima, N.; Yoshihara, K. *J. Chem. Phys.* **1983**, *79*, 2727.
9. Abel, B.; Herzog, B.; Hippler, H.; Troe, J. *J. Chem. Phys*. **1989**, *91*, 900.
10. Tam, A. C.; Sontag, H.; Hess, P. *Chem. Phys. Lett.* **1985**, *120*, 280.
11. Wallington, T. J.; Scheer, M. D.; Braun, W. *Chem. Phys. Lett.* **1987**, *138*, 538.
12. Beck, K. M.; Gordon, R. J. *J. Chem. Phys.* **1987**, *87*, 5681.
13. For a review, see Hsu, H. C.; Tsai, M.-T.; Dyakov, Y. A.; Ni, C.-K. *Int. Rev. Phys. Chem.* **2012**, *31*, 201.
14. Gilbert, R. G. *J. Chem. Phys.* **1984**, *80*, 5501.
15. Toselli, B. M.; Barker, J. R. *Chem. Phys. Lett.* **1990**, *174*, 304.
16. Lim, K. F. *J. Chem. Phys.* **1994**, *101*, 8756.
17. Wright, S. M. A.; Sims, I. R.; Smith, I. W. M. *J. Phys. Chem. A* **2000**, *104*, 10347.
18. Kable, S. H.; Knight, A. E. W. *J Phys. Chem. A*, **2003**, *107*, 10813.
19. For a review, see Zhang, J. Z. H.; Li, Y. M.; Wang, M. L.; Xiang, Y. *Adv. Ser. Phys. Chem.* **2004**, *14*, 209.
20. Fu, B.; Han, Y.-C.; Bowman, J. M.; Leonori, F.; Balucani, N.; Angelucci, L.; Occhiogrosso, A.; Petrucci, R.; Casavecchia, P. *J. Chem. Phys.* **2012**, *137*, 22A532.
21. Dagdigian, P. J. *Int. Rev. Phys. Chem.* **2013**, *32*, 229.
22. Ree, J.; Kim, S. H.; Lee, S. K. J. *Bull. Kor. Chem. Soc.* **2013**, *34*, 1494.
23. Toselli, B. M.; Brenner, J. D.; Yerram, M. L.; Chin, W. E.; King, K. D.; Barker, J. R. *J. Chem. Phys.* **1991**, *95*, 176.
24. Damm, M.; Deckert, F.; Hippler, H.; Troe, J. *J. Phys. Chem.* **1991**, *95*, 2005.
25. Lenzer, T.; Luther, K.; Troe, J.; Gilbert, R. G.; Lim, K. F. *J. Chem. Phys.* **1995**, *103*, 626.
26. Bernshtein, V.; Lim, K. F.; Oref, I. *J. Phys. Chem.* **1995**, *99*, 4531.
27. Shin, H. K. *J. Phys. Chem. A* **2000**, *104*, 6699.
28. Elioff, M. S.; Fang, M.; Mullin, A. S. *J. Chem. Phys.* **2001**, *115*, 6990.
29. Ree, J.; Kim, Y. H.; Shin, H. K. *J. Chem. Phys.* **2002**, *116*, 4858.
30. Ree, J.; Kim, Y. H.; Shin, H. K. *Chem. Phys. Lett.* **2004**, *394*, 250.
31. Ree, J.; Kim, S. H.; Lee, T. H.; Kim, Y. H. *Bull. Kor. Chem. Soc.* **2006**, *27*, 495.
32. (a) Hippler, H.; Troe, J.; Wendelken, H. J. *Chem. Phys. Lett.* **1981**, *84*, 257. (b) *J. Chem. Phys.* **1983**, *78*, 5351; *78*, 6709; *78*, 6718. (c) *ibid* **1984**, *80*, 1853.
33. (a) Bernshtein, V.; Oref, I. *J. Phys. Chem. A* **2006**, *110*, 8477. (b) *J. Phys. Chem. B* **2005**, *109*, 8310. (c) *J. Phys. Chem. A* **2006**, *110*, 1541.
34. Berkowitz, J.; Ellison, G. B.; Gutman, D. *J. Phys. Chem.* **1994**, *98*, 2744.
35. Weast, R. C., Ed., *CRC Handbook of Chemistry and Physics*, 67th ed., CRC Press; Boca Raton, FL: 1986 see p. F-194.
36. Barone, V.; Fliszar, S. *J. Mol. Struc.* (*Theochem*) **1996**, *369*, 29.
37. Guan, Y.; Thompson, D. L. *J. Chem. Phys.* **1990**, *92*, 313.
38. Lapouge, C.; Cavagnat, D. *J. Phys. Chem. A* **1998**, *102*, 8393.
39. Kjaergaard, H. G.; Turbull, D. M.; Henry, B. R. *J. Phys. Chem. A* **1997**, *101*, 2589.
40. Kjaergaard, H. G.; Turnbull, D. M.; Henry, B. R. *J. Phys. Chem. A* **1998**, *102*, 6095.
41. Lim, K. F. *J. Chem. Phys.* **1994**, *100*, 7385.
42. Hirschfelder, J. O.; Curtiss, C. F.; Bird, R. B. *Molecular Theory of Gases and Liquids*; Wiley: New York, 1967; see p. 168 for the combining laws, pp. 1110-1112 and 1212-1214 for *D* and *a*, respectively.
43. Xie, Y.; Boggs, J. E. *J. Comp. Chem.* **1986**, *7*, 158.
44. http://webbook.nist.gov/chemistry/name-ser.html (Accessed Aug. 13, 2013)
45. Olney, T. N.; Cann, N. M.; Cooper, G.; Brion, C. E. *Chem. Phys.* **1997**, *223*, 59.
46. Huber, K. P.; Herzberg, G. *Constants of Diatomic Molecules*; Van Nostrand Reinhold: New York, 1979.
47. Gear, C. W. *Numerical Initial Value Problems in Ordinary Differential Equations*; Prentice-Hall: New York, 1971.
48. MATH/LIBRARY, *Fortran Subroutines for Mathematical Applications*; IMSL: Houston, 1989; p 640.